SU(3) breaking effect in the Z_c and Z_{cs} states

Kan Chen[*]

School of Physics, Northwest University, Xi'an 710127, China;
Shaanxi Key Laboratory for Theoretical Physics Frontiers, Xi'an 710127, China;
Institute of Modern Physics, Northwest University, Xi'an 710127, China;
Peng Huanwu Center for Fundamental Theory, Xi'an 710127, China;
and School of Physics and Center of High Energy Physics, Peking University,
Beijing 100871, China

Based on the hadronic resonance picture, we explore a unified framework to describe the observed Z_{cs} and Z_c states that are close to the thresholds of the $D^{(*)}\bar{D}_s^{(*)}$ and $D^{(*)}\bar{D}^{(*)}$ systems, respectively. We assume that the $Z_{cs}(4000)$ and $Z_{cs}(3985)$ are two different states. Specifically, we assign the $Z_{cs}(4000)$ as the SU(3) partner of the $Z_c(3900)$ ($J^{PC} = 1^{+-}$) due to its observation in the $J/\Psi K$ channel, the difficulty of this assignment is the large width difference between the $Z_{cs}(4000)$ and the $Z_c(3900)$ state. Then the $Z_{cs}(3985)$ should corresponds to the Z_c state that is close to the threshold of $D\bar{D}^*$ system with $J^{PC} = 1^{++}$, the difficulty of this assignment is the absence of such a Z_c state in experiment. We construct the effective potentials of the Z_{cs} and Z_c states by analogy with the effective potentials of the leading-order and next-to-leading-order $N - \bar{N}$ interactions. Then we introduce an SU(3) breaking factor g_x to identify the differences between the effective potentials in the Z_{cs} and Z_c states. We perform two calculations to discuss the differences and similarities of the Z_{cs} and Z_c states. In the first calculation, we show that the above two difficulties can be explained simultaneously by the inclusion of the SU(3) breaking effect. In the second calculation, we show that this framework is promising to simultaneously describe the interactions of the observed Z_{cs} and Z_c states that are close to the thresholds of the $D^{(*)}\bar{D}_s^{(*)}$ and $D^{(*)}\bar{D}^{(*)}$ systems, respectively.

I. INTRODUCTION

In recent years, several charged hidden charm states that are close to the thresholds of the $D^{(*)}\bar{D}_s^{(*)}$ and $D^{(*)}\bar{D}^{(*)}$ systems are discovered in various experiments [1–9]. In Table I, we list their masses, widths, and observed channels. These states have exotic quantum numbers; the identifications of their exotic natures are straightforward. Their possible underlying structures are extensively discussed in many literatures (see reviews [10–21]).

In the Z_c sector, the spin-parity number of $Z_c(3900)$ is measured to be 1^+ [22]. The spin-parity number of $Z_c(4020)$ [1] is not measured yet, but since the masses of $Z_c(3900)$ and $Z_c(4020)$ are above the thresholds of the $D\bar{D}^*$ and $D^*\bar{D}$ by a few MeV, respectively, they both have narrow widths. Thus, the $Z_c(4020)$ is assumed to be the

heavy quark spin (HQS) partner of the $Z_c(3900)$ and have $J^P = 1^+$.

The states $Z_c(4050)$ [4], $Z_c(4055)$ [9], and $Z_c(4100)$ [7] listed in Table I still need further confirmation. Among them, the $Z_c(4055)$ is reported [9] in the $e^+e^- \rightarrow \pi^+\pi^-\Psi(2S)$ via the initial state radiation process. The resonance parameters of the $Z_c(4055)$ are extracted to be $M = 4054 \pm 3 \pm 1$ and $\Gamma = 45 \pm 11 \pm 6$ MeV. However, after taking into account the interference effect between the $\pi^+\pi^-$ amplitude and the Z_c amplitude, further preliminary partial wave analysis (PWA) [23] shows that the resonance parameters of this structure could become $M = 4019.0 \pm 1.9$ and $\Gamma = 29 \pm 4$ MeV, which are consistent with the resonance parameters of $Z_c(4020)$. If such PWA analysis is confirmed, the $Z_c(4020)$ can also decay into $\pi\Psi(2S)$ final states. The $Z_c(4100)^\pm$ [7] is reported in the $B^0 \rightarrow K^+\pi^-\eta_c$ process; the spin-parity assignments $J^P = 1^-$ and 0^+ are both consistent with the data. Besides, the $Z_c(4050)^\pm$ is reported in the $B^0 \rightarrow K^+\pi^-\chi_{c1}$ process [4]. The possible interpretations to the above Z_c states include the molecular states, tetraquark states, and kinematical effects (see reviews [10–21]).

TABLE I. The observed Z_{cs} and Z_c states that are close to the $D^{(*)}\bar{D}_s^{(*)}$ and $D^{(*)}\bar{D}^{(*)}$ thresholds, respectively. The masses and widths are in units of MeV. The statistical and systematical errors have been added in quadrature.

State	$I(J^P)$	Mass	Width	Decay channel
$Z_c(3900)^{\pm}$ [1]	$1^+(1^{+-})$	3887 ± 3	28 ± 3	$J/\Psi\pi$, $D\bar{D}^*$
$Z_c(4020)^{\pm}$ [1]	$1^+(?^{?-})$	4024 ± 2	13 ± 5	$h_c(1P)\pi$, $D^*\bar{D}^*$
$Z_c(4050)^{\pm}$ [4]	$1^-(?^{?+})$	4051^{+24}_{-43}	82^{+52}_{-28}	$\pi^+\chi_{c1}(1P)$
$Z_c(4055)^{\pm}$ [9]	$1^+(?^{?-})$	4054 ± 3	45 ± 13	$\pi^+\Psi(2S)$
$Z_c(4100)^{\pm}$ [7]	$1^-(?^{??})$	4096^{+27}_{-30}	152^{+84}_{-68}	$\eta_c(1S)\pi^-$

State	$I^G(J^{PC})$	Mass	Width	Decay channel
$Z_{cs}(3985)^+$ [2,3]	$\frac{1}{2}(?^?)$	3985 ± 3	14^{+10}_{-7}	$D_s^+\bar{D}^{*0} + D_s^{*+}\bar{D}^0$
$Z_{cs}(4000)^+$ [5,6]	$\frac{1}{2}(1^+)$	4003^{+7}_{-15}	131 ± 30	$J/\Psi K^+$
$Z_{cs}(4123)^-$ [8]	$\frac{1}{2}(?^?)$	4124 ± 5	$\cdots$	$D_s^{*-}D^{*0}$ + c.c.
$Z_{cs}(4220)^+$ [6]	$\frac{1}{2}(1^+)$	4216^{+49}_{-38}	233^{+110}_{-90}	$J/\Psi K^+$

In the Z_{cs} sector, the $Z_{cs}(3985)$ [2,3], $Z_{cs}(4000)$ [5,6], and $Z_{cs}(4220)$ [6] listed in Table I are reported with high significances. On the contrary, due to the low significance, the width of the $Z_{cs}(4123)$ state is not extracted yet [8]; this state still needs further confirmation. The observed exotic Z_{cs} states also have various interpretations, including the molecular states [24–33], tetraquark states [33–41], mixing schemes [42–44], and cusp effects [45]. Since the $Z_{cs}(3985)^+$ and $Z_{cs}(4000)^+$ are both close to the threshold of the $D_s^+\bar{D}^{*0} + D_s^{*+}\bar{D}^0$ system, the question of whether the $Z_{cs}(3985)$ and $Z_{cs}(4000)$ are the same state [27,46,47] or two different ones [26,29,31,37,39,40,43] is still under debate. Particularly, a recent investigation from the BESIII collaboration reported the absence of the $Z_{cs}(3985)$ in the $J/\Psi K$ final states [48]. This result favors the view that the $Z_{cs}(3985)$ and $Z_{cs}(4000)$ are two different states. According to the different observed channels or the heavy quark spin symmetry [29], the $Z_{cs}(4000)$ could be assigned as the $SU(3)_f$ partner of the $Z_c(3900)$. However, such assignment leads to two difficulties:

(1) The width of the $Z_{cs}(4000)$ is about 10 times larger than that of the $Z_c(3900)$.

(2) The SU(3) symmetry requires the existence of a Z_c that is close to the $D\bar{D}^*$ threshold with $J^{PC} = 1^{++}$, this state should be the $SU(3)_f$ partner of the $Z_{cs}(3985)$. However, such state is missing in experiment.

Since the masses of these discussed Z_c and Z_{cs} states are all slightly above their corresponding thresholds in the $D^{(*)}\bar{D}^{(*)}$ and $D^{(*)}\bar{D}_s^{(*)}$ systems, respectively, this important feature leads the molecule resonance picture to become a natural interpretation to these states.

In this work, we assume that the discussed Z_c and Z_{cs} states are resonances composed of the $D^{(*)}\bar{D}^{(*)}$ and $D_s^{(*)}\bar{D}^{(*)}$

components, respectively, and explore a unified effective field theory to describe their masses and widths. The effective potentials of the Z_c and Z_{cs} states are constructed by analogy with the leading-order (LO) and next-to-leading-order (NLO) $N - \bar{N}$ effective potentials [49]. The involved low energy constants (LECs) are determined with the data from the observed Z_c and Z_{cs} states. The effective potentials of the Z_c and Z_{cs} states with different quantum numbers can be related with respect to the HQS and SU(3) flavor symmetry. We will show that this framework is promising for a unified description of the Z_c and Z_{cs} after considering a simplified SU(3) breaking effect. In addition, this SU(3) breaking effect is also crucial to explain the absence of a $J^{PC} = 1^{++}$ Z_c state and the large width difference between the $Z_c(3900)$ and the $Z_{cs}(4000)$.

This paper is organized as follows. We present our theoretical framework in Sec. II. In Sec. III, we present our two calculations to discuss the differences and similarities between the Z_{cs} and Z_c states, we will also present our numerical results and discussions in this section. Section V is a summary.

II. THEORETICAL FRAMEWORK

First, we present the wave functions of the considered Z_{cs} and Z_c systems. In each system, there are six S-wave states, we collectively express them as

$$|D\bar{D}_{(s)}; 0^{+\widetilde{+}}\rangle = |D\bar{D}_{(s)}\rangle_{J=0}, \tag{1}$$

$$|D\bar{D}_{(s)}^*; 1^{+\widetilde{+}}\rangle = (|D\bar{D}_{(s)}^*\rangle_{J=1} + |D^*\bar{D}_{(s)}\rangle_{J=1})/\sqrt{2}, \tag{2}$$

$$|D\bar{D}_{(s)}^*; 1^{+\widetilde{-}}\rangle = (|D\bar{D}_{(s)}^*\rangle_{J=1} - |D^*\bar{D}_{(s)}\rangle_{J=1})/\sqrt{2}, \tag{3}$$

$$|D^*\bar{D}_{(s)}^*; 0^{+\widetilde{+}}\rangle = |D^*\bar{D}_{(s)}^*\rangle_{J=0}, \tag{4}$$

$$|D^*\bar{D}_{(s)}^*; 1^{+\widetilde{-}}\rangle = |D^*\bar{D}_{(s)}^*\rangle_{J=1}, \tag{5}$$

$$|D^*\bar{D}_{(s)}^*; 2^{+\widetilde{+}}\rangle = |D^*\bar{D}_{(s)}^*\rangle_{J=2}. \tag{6}$$

Here, the superscript "~" on the C-parity number is only for the $D^{(*)}\bar{D}_s^{(*)}$ state; since the $D^{(*)}\bar{D}_s^{(*)}$ state does not have the C parity, we use the $|D^{(*)}D_s^{(*)}; J^{P\tilde{C}}\rangle$ to denote that it is the strangeness partner of the $|D^{(*)}\bar{D}^{(*)}; J^{PC}\rangle$ state. The $(|D\bar{D}^*; 1^{+-}\rangle, |D^*\bar{D}^*; 1^{+-}\rangle)$, $(|D\bar{D}_s^*; 1^{+\widetilde{-}}\rangle, |D^*\bar{D}_s^*; 1^{+\widetilde{-}}\rangle)$, $(|D\bar{D}^*; 1^{++}\rangle, |D^*\bar{D}^*; 2^{++}\rangle)$, and $(|D\bar{D}_s^*; 1^{+\widetilde{+}}\rangle, |D^*\bar{D}_s^*; 2^{+\widetilde{+}}\rangle)$ are the four sets of HQS doublets.

Now we construct an effective theory to describe the interactions of the Z_{cs} and Z_c states. We attribute the interactions between the $D^{(*)}$ and $\bar{D}_{(s)}^{(*)}$ mesons to the exchanges of S and P wave light mesons. We omit the

contributions of exchanging charmonium states since their contributions should be suppressed by the masses of $c\bar{c}$ mesons.

The typical forms of the effective potentials of the S-wave and P-wave interactions can be obtained by analogy with the leading-order and next-to-leading-order $N\bar{N}$ interactions. Besides, since we only consider the exchanges of S- and P-wave light mesons, the types of exchanged light mesons only depend on the flavor and spin structures of light quark components in the $D^{(*)}\bar{D}^{(*)}_{(s)}$ system. Thus, we introduce our effective potential at the hadron level in terms of quark-level language.

By analogy with the $N\bar{N}$ interaction [49], we introduce the leading-order contact terms to describe the exchanges of $q\bar{q}$ light mesons in the $D^{(*)}\bar{D}^{(*)}$ and $D^{(*)}\bar{D}^{(*)}_s$ systems:

$$V^{\mathrm{LO}}_{q\bar{q}} = \tilde{g}_s \boldsymbol{F}_1 \cdot \boldsymbol{F}_2 + \tilde{g}_a \boldsymbol{F}_1 \cdot \boldsymbol{F}_2 \boldsymbol{\sigma}_1 \cdot \boldsymbol{\sigma}_2, \quad (7)$$

respectively. Here, the $\boldsymbol{F}_1 \cdot \boldsymbol{F}_2 = -\sum_{l=1}^{8} \lambda_1^l \lambda_2^{*l}$ and $\boldsymbol{\sigma}_1 \cdot \boldsymbol{\sigma}_2 = \sum_{m=1}^{3} \sigma_1^m \sigma_2^m$ are the flavor and spin operators of the light quark components, respectively. The $\tilde{g}_s$ and $\tilde{g}_a$ are the two LO low energy constants (LECs). Note that

$$\boldsymbol{\lambda}_1 \cdot \boldsymbol{\lambda}_2^* = \lambda_1^8 \lambda_2^{*8} + \lambda_1^i \lambda_2^{*i} + \lambda_1^j \lambda_2^{*j}, \quad (8)$$

where i and j sum from 1 to 3 and 4 to 7, respectively. The matrix elements of the operators $\lambda_1^8 \lambda_2^{*8}$ ($\lambda_1^8 \lambda_2^{*8}\boldsymbol{\sigma}_1 \cdot \boldsymbol{\sigma}_2$), $\lambda_1^i \lambda_2^i$ ($\lambda_1^i \lambda_2^{*i}\boldsymbol{\sigma}_1 \cdot \boldsymbol{\sigma}_2$), and $\lambda_1^j \lambda_2^j$ ($\lambda_1^j \lambda_2^{*j}\boldsymbol{\sigma}_1 \cdot \boldsymbol{\sigma}_2$) quantify the fractions of the contributions from the exchanges of the isospin singlet, triplet, and two doublets light scalar (axial-vector) meson currents, respectively.

The effective potential defined in Eq. (7) allows the exchanges of two sets of light mesons with quantum numbers $I(J^P) = 0(0)^+$, $1(0^+)$, $1/2(0^+)$ and $I(J^P) = 0(1^+)$, $1(1^+)$, $1/2(1^+)$. For each exchanged meson current, their spin and flavor structures are identified by the corresponding spin and flavor matrix elements, respectively. Then we use the coupling constants $\tilde{g}_s \approx g_s^2/m_s^2$ and $\tilde{g}_a \approx g_a^2/m_a^2$ to collectively quantify the dynamical effects from the exchange of each scalar and axial-vector meson current [50]. In the SU(3) limit, the couplings $\tilde{g}_s$ ($\tilde{g}_a$) for the exchanges of scalar (axial-vector) meson currents with different isospins are the same.

Then we proceed to introduce the effective potentials of the Z_{cs} and Z_c states at NLO. By analogy with the NLO $N - \bar{N}$ interaction [49], the contact terms that attributed to the exchanges of light mesons in the Z_{cs} and Z_c systems read

$$V^{\mathrm{NLO}}_{q\bar{q}} = (\boldsymbol{F}_1 \cdot \boldsymbol{F}_2)\big[g_1 \boldsymbol{q}^2 + g_2 \boldsymbol{k}^2 + (g_3 \boldsymbol{q}^2 + g_4 \boldsymbol{k}^2)\boldsymbol{\sigma}_1 \cdot \boldsymbol{\sigma}_2$$
$$+ \frac{i}{2} g_5 (\boldsymbol{\sigma}_1 + \boldsymbol{\sigma}_2) \cdot (\boldsymbol{q} \times \boldsymbol{k}) + g_6 (\boldsymbol{q} \cdot \boldsymbol{\sigma}_1)(\boldsymbol{q} \cdot \boldsymbol{\sigma}_2)$$
$$+ g_7 (\boldsymbol{k} \cdot \boldsymbol{\sigma}_1)(\boldsymbol{k} \cdot \boldsymbol{\sigma}_2)\big]. \quad (9)$$

Here, the transferred momentum $\boldsymbol{q} = \boldsymbol{p} - \boldsymbol{p}'$, and the average momentum $\boldsymbol{k}$ is defined by $\boldsymbol{k} = (\boldsymbol{p}' + \boldsymbol{p})/2$. When performing an S-wave channel partial-wave projection, the g_5 term will not contribute to the S-wave potential, and the possible $\boldsymbol{p} \cdot \boldsymbol{p}'$ terms will also vanish, then Eq. (9) can be rewritten as

$$V^{\mathrm{NLO}}_{q\bar{q}} = (\boldsymbol{F}_1 \cdot \boldsymbol{F}_2)(\boldsymbol{p}^2 + \boldsymbol{p}'^2)\big[(\tilde{g}_1 + \tilde{g}_2)$$
$$+ (\tilde{g}_3 + \tilde{g}_4 + \tilde{g}_6 + \tilde{g}_7)(\boldsymbol{\sigma}_1 \cdot \boldsymbol{\sigma}_2)\big]$$
$$= (\boldsymbol{F}_1 \cdot \boldsymbol{F}_2)\big[\tilde{g}_{sp} + \tilde{g}_{ap}(\boldsymbol{\sigma}_1 \cdot \boldsymbol{\sigma}_2)\big](\boldsymbol{p}^2 + \boldsymbol{p}'^2). \quad (10)$$

The LECs $\tilde{g}_{sp} \approx g_{sp}^2/m_{sp}^2$ and $\tilde{g}_{ap} \approx g_{ap}^2/m_{ap}^2$ are introduced to describe the effective couplings of the momentum dependent terms $\boldsymbol{F}_1 \cdot \boldsymbol{F}_2(\boldsymbol{p}^2 + \boldsymbol{p}'^2)$ and $\boldsymbol{F}_1 \cdot \boldsymbol{F}_2(\boldsymbol{\sigma}_1 \cdot \boldsymbol{\sigma}_2)(\boldsymbol{p}^2 + \boldsymbol{p}'^2)$, respectively.

By collecting Eq. (7) with Eq. (10), the total effective potential of the Z_{cs} or Z_c states can be written as

$$V_{Z_{c(s)}} = V^{\mathrm{LO}}_{q\bar{q}} + V^{\mathrm{NLO}}_{q\bar{q}}. \quad (11)$$

This effective potential includes four LECs, i.e., the $\tilde{g}_s$, $\tilde{g}_a$, $\tilde{g}_{sp}$, and $\tilde{g}_{ap}$; we will determine them in the next section.

III. NUMERICAL RESULTS AND DISCUSSIONS

In this section, we first introduce our scheme to include the SU(3) breaking effect in the Z_{cs} and Z_c states, then we will perform two calculations to compare the differences and similarities of the observed Z_{cs} and Z_c states in Secs. III B and III C, respectively.

A. SU(3) breaking factor g_x

In Table II, for the considered Z_{cs} and Z_c states, we list their matrix elements of the operators,

$$\mathcal{O}_1 = \sum_{i=1}^{7} \lambda_1^i \cdot \lambda_2^{*i}, \qquad \mathcal{O}_2 = \lambda_1^8 \cdot \lambda_2^{*8},$$
$$\mathcal{O}_3 = \sum_{i=1}^{7} \lambda_1^i \cdot \lambda_2^{*i}\boldsymbol{\sigma}_1 \cdot \boldsymbol{\sigma}_2, \qquad \mathcal{O}_4 = \lambda_1^8 \lambda_2^{*8}\boldsymbol{\sigma}_1 \cdot \boldsymbol{\sigma}_2.$$

We can write out the effective potential of a specific Z_{cs} or Z_c state from Table II and Eq. (11).

As presented in Table II, on the one hand, in the SU(3) limit, the Z_c and Z_{cs} states with the same quantum numbers share identical matrix elements $\langle\mathcal{O}_1\rangle + \langle\mathcal{O}_2\rangle$ and $\langle\mathcal{O}_3\rangle + \langle\mathcal{O}_4\rangle$. Correspondingly, the Z_c and Z_{cs} states with the same $J^{P\tilde{C}}$ share identical effective potential; this is the requirement from the SU(3) flavor symmetry.

On the other hand, in the Z_{cs} states, the matrix elements $\mathcal{O}_1$ and $\mathcal{O}_3$ vanish, the total effective potentials of the Z_{cs} states consist of the operators $\mathcal{O}_2$ ($\lambda_1^8 \cdot \lambda_2^{*8}$) and $\mathcal{O}_4$ ($\lambda_1^8 \cdot \lambda_2^{*8}\boldsymbol{\sigma}_1 \cdot \boldsymbol{\sigma}_2$). They correspond to the interactions from

TABLE II. The matrix elements of the operators $\mathcal{O}_1$ $(\sum_{i=1}^{7}\lambda_1^i \cdot \lambda_2^{*i})$ $\mathcal{O}_2$ $(\lambda_1^8 \cdot \lambda_2^{*8})$, $\mathcal{O}_3$ $(\sum_{i=1}^{7}\lambda_1^i \cdot \lambda_2^{*i}\boldsymbol{\sigma}_1 \cdot \boldsymbol{\sigma}_2)$, $\mathcal{O}_4$ $(\lambda_1^8 \lambda_2^{*8}\boldsymbol{\sigma}_1 \cdot \boldsymbol{\sigma}_2)$ in the Z_c $(D^{(*)}\bar{D}^{(*)})$ and Z_{cs} $(D^{(*)}\bar{D}_s^{(*)})$ states. Here, we use the notation $|D^{(*)}\bar{D}_s^{(*)};J^{P\widetilde{C}}\rangle$ to denote that it is the strangeness partner of the $|D^{(*)}\bar{D}^{(*)};J^{PC}\rangle$ state.

State	$\mathcal{O}_1$	$\mathcal{O}_2$	$\mathcal{O}_3$	$\mathcal{O}_4$	State	$\mathcal{O}_1$	$\mathcal{O}_2$	$\mathcal{O}_3$	$\mathcal{O}_4$
$|D\bar{D};0^{++}\rangle$	1	$-\frac{1}{3}$	0	0	$|D\bar{D}_s;0^{+\widetilde{+}}\rangle$	0	$\frac{2}{3}$	0	0
$|D\bar{D}^*;1^{++}\rangle$	1	$-\frac{1}{3}$	1	$-\frac{1}{3}$	$|D\bar{D}_s^*;1^{+\widetilde{+}}\rangle$	0	$\frac{2}{3}$	0	$\frac{2}{3}$
$|D\bar{D}^*;1^{+-}\rangle$	1	$-\frac{1}{3}$	-1	$\frac{1}{3}$	$|D\bar{D}_s^*;1^{+\widetilde{-}}\rangle$	0	$\frac{2}{3}$	0	$-\frac{2}{3}$
$|D^*\bar{D}^*;0^{++}\rangle$	1	$-\frac{1}{3}$	-2	$\frac{2}{3}$	$|D^*\bar{D}_s^*;0^{+\widetilde{+}}\rangle$	0	$\frac{2}{3}$	0	$-\frac{4}{3}$
$|D^*\bar{D}^*;1^{+-}\rangle$	1	$-\frac{1}{3}$	-1	$\frac{1}{3}$	$|D^*\bar{D}_s^*;1^{+\widetilde{-}}\rangle$	0	$\frac{2}{3}$	0	$-\frac{2}{3}$
$|D^*\bar{D}^*;2^{++}\rangle$	1	$-\frac{1}{3}$	1	$-\frac{1}{3}$	$|D^*\bar{D}_s^*;2^{+\widetilde{+}}\rangle$	0	$\frac{2}{3}$	0	$\frac{2}{3}$

the exchanges of light mesons with $n\bar{n} + s\bar{s}$ ($n = u$, d) components. In the Z_c states, their effective potentials have nonzero contributions from the operators $\mathcal{O}_1$ $(\sum_{i=1}^{7}\lambda_1^i \cdot \lambda_2^{*i})$ and $\mathcal{O}_3$ $(\sum_{i=1}^{7}\lambda_1^i \cdot \lambda_2^{*i}\boldsymbol{\sigma}_1 \cdot \boldsymbol{\sigma}_2)$ (except the $\langle\mathcal{O}_3\rangle = 0$ in the $|D\bar{D};0^{++}\rangle$ state). Specifically, the matrix elements in the operators $\mathcal{O}_1$ and $\mathcal{O}_3$ with $i = 1$, 2, 3 are nonzero; they correspond to the interactions from the exchanges of $n\bar{n}$ ($n = u$, d) light mesons, while the matrix elements in the operators $\mathcal{O}_1$ and $\mathcal{O}_3$ with $i = 4$, 5, 6, 7 are zero; they correspond to the interactions from the exchanges of $n\bar{s}/s\bar{n}$ strange mesons.

To include the SU(3) breaking effects between the Z_{cs} and Z_c states, from the effective potentials listed in Table II, we adopt the following approximation:

$$m_i < m_8. \qquad (12)$$

Here, the m_i and m_8 denote the masses of exchanged light mesons that are related to the flavor isospin triplet $\sum_{i=1}^{3}\lambda_1^i \cdot \lambda_2^i$ and isospin singlet $\lambda_1^8 \cdot \lambda_2^{*8}$ operators, respectively. Comparing to the effective coupling constants $\tilde{g}_s$, $\tilde{g}_a$, $\tilde{g}_{sp}$, $\tilde{g}_{ap}$ that are related to the $\lambda_1^8 \cdot \lambda_2^8$ and proportional to $1/m_8^2$, the effective coupling constants $\tilde{g}'_s$, $\tilde{g}'_a$, $\tilde{g}'_{sp}$, $\tilde{g}'_{ap}$ that are related to the $\lambda_1^i \cdot \lambda_2^{*i}$ operator are magnified by $1/m_i^2$, i.e.,

$$\tilde{g}_s = \frac{g_s^2}{m_{s8}^2} < \tilde{g}'_s = \frac{g_s^2}{m_{si}^2}, \qquad (13)$$

$$\tilde{g}_a = \frac{g_a^2}{m_{a8}^2} < \tilde{g}'_a = \frac{g_a^2}{m_{ai}^2}, \qquad (14)$$

$$\tilde{g}_{sp} = \frac{g_{sp}^2}{m_{sp8}^2} < \tilde{g}'_{sp} = \frac{g_{sp}^2}{m_{spi}^2}, \qquad (15)$$

$$\tilde{g}_{ap} = \frac{g_{ap}^2}{m_{ap8}^2} < \tilde{g}'_{ap} = \frac{g_{ap}^2}{m_{api}^2}. \qquad (16)$$

In principle, the SU(3) breaking effects should be slightly different among the four interacting terms that are related to the $\tilde{g}_s/\tilde{g}'_s, \tilde{g}_a/\tilde{g}'_a, \tilde{g}_{sp}/\tilde{g}'_{sp}, \tilde{g}_{ap}/\tilde{g}'_{ap}$ couplings. At present, we do not have enough data to specify such differences. Instead, we introduce a global SU(3) breaking factor g_x, and redefine the coupling parameters $\tilde{g}'_s, \tilde{g}'_a, \tilde{g}'_{sp}, \tilde{g}'_{ap}$ that are related to the exchanges of the isospin triplet light mesons as

$$\tilde{g}'_s = g_x\tilde{g}_s, \quad \tilde{g}'_a = g_x\tilde{g}_a, \quad \tilde{g}'_{sp} = g_x\tilde{g}_{sp}, \quad \tilde{g}'_{ap} = g_x\tilde{g}_{ap}. \quad (17)$$

According to Eqs. (13)–(16), the factor g_x is expected to have $g_x > 1$.

B. The differences of the Z_{cs} and Z_c states

After identifying the SU(3) breaking effect, we present our first calculation to clarify the differences between the Z_{cs} and Z_c states. Here, we need to pin down the five coupling parameters, i.e., the $\tilde{g}_s$, $\tilde{g}_a$, $\tilde{g}_{sp}$, $\tilde{g}_{ap}$, and g_x, while the $\tilde{g}'_s$, $\tilde{g}'_a$, $\tilde{g}'_{sp}$, $\tilde{g}'_{ap}$ can be obtained from the above five parameters as redefined in Eq. (17).

The $Z_{cs}(3985)$ [2,3] and $Z_{cs}(4000)$ [5,6] are reported in the $D_s^+\bar{D}^{*0} + D_s^{*+}\bar{D}^0$ $(D_s^+D^{*-} + D_s^{*+}D^-)$ and $J/\Psi K^+$ $(J/\Psi K_S^0)$ final states, respectively. In this work, we treat the $Z_{cs}(4000)$ and $Z_{cs}(3985)$ as two different states. According to the heavy quark spin symmetry [29], the $|D\bar{D}_s^*;1^{+\widetilde{+}}\rangle$ state cannot decay into the $J/\Psi K^+$ final states. Thus, we assume the following assignments:

Set 1: $Z_{cs}(4000)|D\bar{D}_s^*;1^{+\widetilde{-}}\rangle$, $\qquad Z_{cs}(3985)|D\bar{D}_s^*;1^{+\widetilde{+}}\rangle$.

We denote this set of assignments as set 1. From Table II, we can directly obtain the effective potentials of the $Z_{cs}(4000)$ and $Z_{cs}(3985)$ as

$$V_{Z_{cs}(4000)} = \frac{2}{3}(\tilde{g}_s - \tilde{g}_a) + \frac{2}{3}(\tilde{g}_{sp} - \tilde{g}_{ap})(p^2 + p'^2), \quad (18)$$

$$V_{Z_{cs}(3985)} = \frac{2}{3}(\tilde{g}_s + \tilde{g}_a) + \frac{2}{3}(\tilde{g}_{sp} + \tilde{g}_{ap})(p^2 + p'^2). \quad (19)$$

As presented in Table II, the matrix elements $\langle\mathcal{O}_1\rangle$ and $\langle\mathcal{O}_3\rangle$ vanish in the Z_{cs} states; thus, we do not need to introduce the g_x to describe the effective potentials of the Z_{cs} states with different quantum numbers.

By introducing the experimental masses and widths of the $Z_{cs}(4000)$ and $Z_{cs}(3985)$, we can solve the LECs $(\tilde{g}_s, \tilde{g}_a, \tilde{g}_{sp}, \tilde{g}_{ap})$ with the following Lippmann-Schwinger equation:

$$T(\boldsymbol{p'},\boldsymbol{p}) = V(\boldsymbol{p'},\boldsymbol{p}) + \int \frac{d^3\boldsymbol{q}}{(2\pi)^3}\frac{V(\boldsymbol{p'},\boldsymbol{q})T(\boldsymbol{q},\boldsymbol{p})u^2(\Lambda)}{E - \sqrt{m_1^2 + \boldsymbol{q}^2} + \sqrt{m_2^2 + \boldsymbol{q}^2}}, \quad (20)$$

where m_1 and m_2 are the masses of the charmed and charmed-strange meson components in the Z_{cs} states. To

suppress the contributions from high momenta, we introduce a dipole form factor $u(\Lambda) = (1 + q^2/\Lambda^2)^{-2}$.

In the view of chiral effective field theory [49,51–53], the light hadron ρ and other higher states are treated as the hard scale and integrated out. This imposes the restriction that the cutoff value Λ should be smaller than the m_ρ. However, in the present framework, the exchanged light mesons may include the scalar, axial-vector, pseudoscalar, and vector mesons; thus, we select a moderate value with $\Lambda = 1.0$ GeV [50,54–56] to perform our calculation. We will discuss the Λ dependences of our results in Sec. III C.

For the separable effective potentials in Eqs. (18) and (19), we solve the above Lippmann-Schwinger equation with the matrix-inversion method [57]. The conditions that the poles of the $|D\bar{D}_s^*; 1^{+-}\rangle$ and $|D\bar{D}_s^*; 1^{+-}\rangle$ states can coexist are

$$\text{Det}\left[\begin{pmatrix} 1 & 0 \\ 0 & 1 \end{pmatrix} - \begin{pmatrix} A & B \\ B & 0 \end{pmatrix}\begin{pmatrix} G_0 & G_2 \\ G_2 & G_4 \end{pmatrix}\right] = 0, \quad (21)$$

$$\text{Det}\left[\begin{pmatrix} 1 & 0 \\ 0 & 1 \end{pmatrix} - \begin{pmatrix} C & D \\ D & 0 \end{pmatrix}\begin{pmatrix} G_0 & G_2 \\ G_2 & G_4 \end{pmatrix}\right] = 0, \quad (22)$$

with $A = \frac{2}{3}(\tilde{g}_s - \tilde{g}_a)$, $B = \frac{2}{3}(\tilde{g}_{sp} - \tilde{g}_{ap})$, $C = \frac{2}{3}(\tilde{g}_s + \tilde{g}_a)$, and $D = \frac{2}{3}(\tilde{g}_{sp} + \tilde{g}_{ap})$. Here, G_n is defined as

$$G_n = \int \frac{1}{2\pi^2} \frac{q^{2+n}(1 + \frac{q^2}{\Lambda})^{-4}}{E - \sqrt{m_1^2 + q^2} - \sqrt{m_2^2 + q^2}}. \quad (23)$$

We replace the integration variable q with $q \to q \times \exp(-i\theta)$, and set $0 < \theta < \frac{\pi}{2}$ to search for the $|D\bar{D}_s^*; 1^{+-}\rangle$ and $|D^*\bar{D}_s^*; 1^{++}\rangle$ resonances in the second Riemann sheet. By adopting the experimental central values of the $Z_{cs}(4000)$ [6] and $Z_{cs}(3985)$ [2], the four LECs are obtained as

$$\tilde{g}_s = 32.1 \text{ GeV}^{-2}, \qquad \tilde{g}_a = 20.8 \text{ GeV}^{-2}, \quad (24)$$

$$\tilde{g}_{sp} = -61.5 \text{ GeV}^{-4}, \qquad \tilde{g}_{ap} = -22.8 \text{ GeV}^{-4}. \quad (25)$$

As presented in Eq. (17), in the Z_c system, we introduce a factor g_x to redefine the LECs ($\tilde{g}_s$, $\tilde{g}_a$, $\tilde{g}_{sp}$, $\tilde{g}_{ap}$) that are related to the operators $\mathcal{O}_2$ and $\mathcal{O}_4$, this factor is only related to the effective potentials of Z_c states. Explicitly, the effective potentials of $|D\bar{D}^*; 1^{+-}\rangle$ ($Z_c(3900)$) and $|D\bar{D}^*; 1^{++}\rangle$ states can be written as

$$V_{|D\bar{D}^*;1^{+-}\rangle} = \left(g_x - \frac{1}{3}\right)(\tilde{g}_s - \tilde{g}_a)$$
$$+ \left(g_x - \frac{1}{3}\right)(\tilde{g}_{sp} - \tilde{g}_{ap})(p^2 + p'^2), \quad (26)$$

$$V_{|D\bar{D}^*;1^{++}\rangle} = \left(g_x - \frac{1}{3}\right)(\tilde{g}_s + \tilde{g}_a)$$
$$+ \left(g_x - \frac{1}{3}\right)(\tilde{g}_{sp} + \tilde{g}_{ap})(p^2 + p'^2). \quad (27)$$

In the HQS limit, the $|D^*\bar{D}^*; 1^{+-}\rangle$ [we assume this state corresponds to the $Z_c(4020)$] and $|D^*\bar{D}^*; 2^{++}\rangle$ share identical effective potentials to that of the $|D\bar{D}^*; 1^{+-}\rangle$ and $|D\bar{D}^*; 1^{++}\rangle$ states, respectively. Thus, we no longer list the effective potentials of the $|D^*\bar{D}^*; 1^{+-}\rangle$ and $|D^*\bar{D}^*; 2^{++}\rangle$ states further.

To pin down the SU(3) breaking factor g_x, we adopt the obtained four LECs extracted from the $Z_{cs}(4000)$ and $Z_{cs}(3985)$ states to the effective potentials of the $(|D\bar{D}^*; 1^{+-}\rangle, |D^*\bar{D}^*; 1^{+-}\rangle)$ and $(|D\bar{D}^*; 1^{++}\rangle, |D^*\bar{D}^*; 2^{++}\rangle)$ states, we run the g_x in a reasonable region, then we check the behaviors of the masses and widths of these two sets of HQS doublets. We find the possible g_x region by reproducing the experimental resonance parameters [1] of the $Z_c(3900)$ [or the $Z_c(4020)$].

The g_x dependences of the masses and widths of the $(|D\bar{D}^*; 1^{+-}\rangle, |D^*\bar{D}^*; 1^{+-}\rangle)$ and $(|D\bar{D}^*; 1^{++}\rangle, |D^*\bar{D}^*; 2^{++}\rangle)$ doublets are presented in Fig. 1. As discussed in Sec. III A, the SU(3) breaking factor g_x is expected to be greater than 1; here, in order to show the evolutions of the masses and widths of these two sets of HQS doublets with g_x, we run g_x from 0.9, slightly smaller than its lower limit.

We first discuss the results in the SU(3) limit at $g_x = 1.0$. As listed in Table III, the obtained resonance parameters of the Z_c states with $J^{PC} = 1^{+-}$ and 1^{++} are very similar to that of the observed $Z_{cs}(4000)$ and $Z_{cs}(3985)$ states, respectively. Here, $\delta_{M-M_{\text{Tr}}}$ is defined as $\delta_{M-M_{\text{Tr}}} = M - M_{\text{Tr}}$, M is the mass of the considered Z_c/Z_{cs} state, and M_{Tr} is the corresponding two-meson threshold. The similarities of $\delta_{M-M_{\text{Tr}}}$ and widths between the $|DD^*; 1^{++}\rangle$ ($|DD^*; 1^{+-}\rangle$) and $|DD_s^*; 1^{++}\rangle$ ($|DD_s^*; 1^{+-}\rangle$) states are exactly the requirements from the SU(3) flavor symmetry.

Then we divide two g_x regions, i.e., the region 1 (green band) and region 2 (yellow band) in Fig. 1 to discuss our results. The smaller and bigger g_x values in region 1 and region 2 denote the tiny and considerable SU(3) breaking effects, respectively. The g_x dependences of the masses and widths of the $(|D\bar{D}^*; 1^{+-}\rangle, |D\bar{D}^*; 1^{++}\rangle)$ states are presented in Figs. 1(a) and 1(b), respectively. As shown in Fig. 1(a), in region 1, where only a tiny SU(3) breaking effect is introduced, a lighter and narrower $|D\bar{D}^*; 1^{++}\rangle$ and a heavier and broader $|D\bar{D}^*; 1^{+-}\rangle$ state can coexist. Besides, the masses of the $|DD^*; 1^{++}\rangle$ and $|DD^*; 1^{+-}\rangle$ have different g_x-dependent behaviors. As the g_x increase, the mass of the $|D\bar{D}^*; 1^{+-}\rangle$ state decreases slowly and can cross region 1, while the mass of the $|D\bar{D}^*; 1^{++}\rangle$ state decreases and moves to the threshold of $D\bar{D}^*$ rapidly. As the mass of $|D\bar{D}^*; 1^{++}\rangle$ state is equal to the threshold of
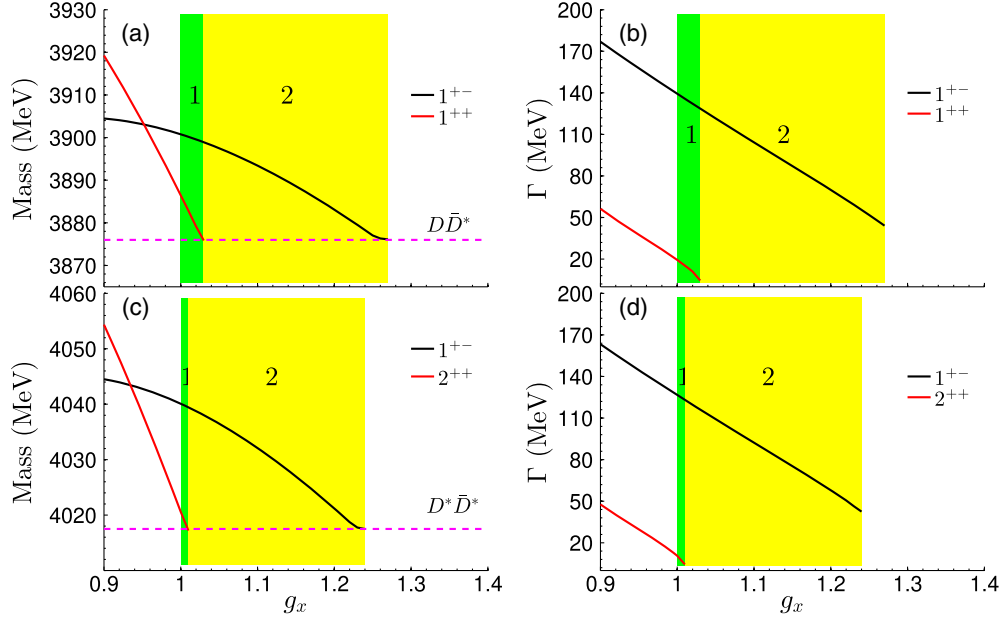
FIG. 1.   The g_x dependences of the masses and widths of the $(|D\bar{D}^*; 1^{+-}\rangle, |D^*\bar{D}^*; 1^{+-}\rangle)$ (black lines) and $(|D\bar{D}^*; 1^{++}\rangle, |D^*\bar{D}^*; 2^{++}\rangle)$ (red lines) doublets. The LECs are extracted from the experimental inputs in set 1.

$D\bar{D}^*$ (the g_x is at the upper limit of region 1), we can no longer find the $|D\bar{D}^*; 1^{++}\rangle$ state in the second Riemann sheet.

At $g_x > 1.03$, we move to region 2, where only the $|D\bar{D}^*; 1^{+-}\rangle$ state can be found in the second Riemann sheet. We find that the width of the $|D\bar{D}^*; 1^{+-}\rangle$ decreases from 128 to 48 MeV as the factor g_x increases from 1.03 to 1.26, respectively. This result shows that a considerable SU(3) breaking can lead the width of the $|D\bar{D}^*; 1^{+-}\rangle$ state to become much smaller.

The above discussions show that our framework provides possible explanations to the absence of the $|D\bar{D}^*; 1^{++}\rangle$ state and the large width difference between the $Z_c(3900)$ and $Z_{cs}(4000)$ states. These two questions are not expected from the SU(3) flavor symmetry but can be solved simultaneously by introducing a considerable SU(3) breaking effect. The $|D^*\bar{D}^*; 1^{+-}\rangle$ and $|D^*\bar{D}^*; 2^{++}\rangle$ are the HQS partners of the $|D\bar{D}^*; 1^{+-}\rangle$ and $|D\bar{D}^*; 1^{++}\rangle$ states, respectively. Their masses and widths have very similar g_x dependences to

that of the $|D\bar{D}^*; 1^{+-}\rangle$ and $|D\bar{D}^*; 1^{++}\rangle$ states, respectively. We illustrate them in Figs. 1(c) and 1(d).

Although the obtained width of the $Z_c(3900)$ in region 2 is still larger than the PDG [1] average value 28.4 ± 2.6 MeV, we need to emphasize that in this calculation, we use the central values of the resonance parameters of the $Z_{cs}(4000)$ [6] and $Z_{cs}(3985)$ [2]; these inputs still have considerable experimental uncertainties, and further measurements on the resonance parameters of the $Z_{cs}(3985)$ and $Z_{cs}(4000)$ from other experiments or processes will provide important guidance to our model.

C. The similarities of the Z_{cs} and Z_c states

Then we proceed to investigate the similarities of the Z_{cs} and Z_c states. In this subsection, within the same framework, we use another scheme to compare the Z_c and Z_{cs} states.

As discussed in Sec. III A, from Table II, the effective potentials of the Z_{cs} states only consist of the exchanges of the isospin singlet light mesons, while the effective potentials of the Z_c states consist of the exchanges of the isospin singlet and isospin triplet light mesons. In the SU(3) limit, the coupling parameters $(\tilde{g}_s, \tilde{g}_a, \tilde{g}_{sp}, \tilde{g}_{ap})$ for the exchange of isospin singlet light mesons should be identical to that of the isospin triplet light mesons.

We introduce the SU(3) breaking effect by multiplying the isospin triplet couplings $\tilde{g}_s$, $\tilde{g}_a$, $\tilde{g}_{sp}$, and $\tilde{g}_{ap}$ with the SU(3) breaking factor g_x, then the explicit expressions of the effective potentials of the considered Z_{cs} and Z_c states are

TABLE III.   The comparison of the masses and widths between the Z_c and Z_{cs} states with $J^{P\tilde{C}} = 1^{+\tilde{\pm}}$. We adopt the LECs solved from the inputs in set 1 to calculate the Z_c states. The SU(3) breaking factor g_x is fixed at 1.0 in the SU(3) limit.

State	Mass (MeV)	$\delta_{M-M_{\mathrm{Tr}}}$ (MeV)	Width (MeV)
$|DD^*; 1^{++}\rangle$	3886.5	10.7	19.4
$|DD_s^*; 1^{++}\rangle$	3985.2	5.9	13.8
$|DD^*; 1^{+-}\rangle$	3900.1	24.3	139.3
$|DD_s^*; 1^{+-}\rangle$	4003.0	23.7	131.0

$$V_{|D\bar{D}_s;0^{++}\rangle}^{\sim} = \frac{2}{3}\left[\tilde{g}_s + \tilde{g}_{sp}A(p,p')\right], \qquad (28)$$

$$V_{|D\bar{D}_s^*;1^{++}\rangle}^{\sim} = \frac{2}{3}\left[(\tilde{g}_s + \tilde{g}_a) + (\tilde{g}_{sp} + \tilde{g}_{ap})A(p,p')\right], \qquad (29)$$

$$V_{|D\bar{D}_s^*;1^{+-}\rangle}^{\sim} = \frac{2}{3}\left[(\tilde{g}_s - \tilde{g}_a) + (\tilde{g}_{sp} - \tilde{g}_{ap})A(p,p')\right], \qquad (30)$$

$$V_{|D^*\bar{D}_s^*;0^{++}\rangle}^{\sim} = \frac{2}{3}\left[(\tilde{g}_s - 2\tilde{g}_a) + (\tilde{g}_{sp} - 2\tilde{g}_{ap})A(p,p')\right], \qquad (31)$$

$$V_{|D^*\bar{D}_s^*;1^{+-}\rangle}^{\sim} = \frac{2}{3}\left[(\tilde{g}_s - \tilde{g}_a) + (\tilde{g}_{sp} - \tilde{g}_{ap})A(p,p')\right], \qquad (32)$$

$$V_{|D^*\bar{D}_s^*;2^{++}\rangle}^{\sim} = \frac{2}{3}\left[(\tilde{g}_s + \tilde{g}_a) + (\tilde{g}_{sp} + \tilde{g}_{ap})A(p,p')\right], \qquad (33)$$

and

$$V_{|D\bar{D};0^{++}\rangle}^{\sim} = g'_x\left[\tilde{g}_s + \tilde{g}_{sp}A(p,p')\right], \qquad (34)$$

$$V_{|D\bar{D}^*;1^{++}\rangle}^{\sim} = g'_x\left[(\tilde{g}_s + \tilde{g}_a) + (\tilde{g}_{sp} + \tilde{g}_{ap})A(p,p')\right], \qquad (35)$$

$$V_{|D\bar{D}^*;1^{+-}\rangle}^{\sim} = g'_x\left[(\tilde{g}_s - \tilde{g}_a) + (\tilde{g}_{sp} - \tilde{g}_{ap})A(p,p')\right], \qquad (36)$$

$$V_{|D^*\bar{D}^*;0^{++}\rangle}^{\sim} = g'_x\left[(\tilde{g}_s - 2\tilde{g}_a) + (\tilde{g}_{sp} - 2\tilde{g}_{ap})A(p,p')\right], \qquad (37)$$

$$V_{|D^*\bar{D}^*;1^{+-}\rangle}^{\sim} = g'_x\left[(\tilde{g}_s - \tilde{g}_a) + (\tilde{g}_{sp} - \tilde{g}_{ap})A(p,p')\right], \qquad (38)$$

$$V_{|D^*\bar{D}^*;2^{++}\rangle}^{\sim} = g'_x\left[(\tilde{g}_s + \tilde{g}_a) + (\tilde{g}_{sp} + \tilde{g}_{ap})A(p,p')\right], \qquad (39)$$

respectively. Here, $A(p,p') = p^2 + p'^2$, and $g'_x = g_x - 1/3$. In the SU(3) limit with $g_x = 1$, the effective potentials of the Z_{cs} states in Eqs. (28)–(33) are identical to that of the Z_c states in Eqs. (34)–(39), respectively.

We select two observed Z_{cs} states and label this set of inputs as set 1, and select two observed Z_c states and label this set of inputs as set 2. We run the g_x in a reasonable region, and separately calculate the $(\tilde{g}_s^{cs}, \tilde{g}_a^{cs}, \tilde{g}_{sp}^{cs}, \tilde{g}_{ap}^{cs})$ and $(\tilde{g}_s^c, \tilde{g}_a^c, \tilde{g}_{sp}^c, \tilde{g}_{ap}^c)$ with the inputs defined in sets 1 and 2, respectively.

As can be seen from Eqs. (28)–(39), the differences of the effective potentials between the Z_{cs} states and Z_c states are collectively absorbed into the SU(3) breaking factor g_x. If such a scheme can approximately describe the SU(3) breaking effect between the Z_{cs} and Z_c states, and if we can find the value of the SU(3) breaking factor g_x, then we may expect that the coupling parameters $\tilde{g}_s^{cs}, \tilde{g}_a^{cs}, \tilde{g}_{sp}^{cs}$, and $\tilde{g}_{ap}^{cs}$ determined from the experimental Z_{cs} states defined in set 1 should be roughly consistent with the coupling parameters $\tilde{g}_s^c, \tilde{g}_a^c, \tilde{g}_{sp}^c$, and $\tilde{g}_{ap}^c$ determined from the experimental Z_c states defined in set 2. Thus, we define a quantity χ^2 with

$$\chi^2 = (\tilde{g}_s^c - \tilde{g}_s^{cs})^2 + (\tilde{g}_a^c - \tilde{g}_a^{cs})^2 + (\tilde{g}_{sp}^c - \tilde{g}_{sp}^{cs})^2 + (\tilde{g}_{ap}^c - \tilde{g}_{ap}^{cs})^2, \qquad (40)$$

and find the minimum χ^2 to determine the g_x.

Now we start to perform our calculation. Here, we still select the $Z_{cs}(4000)$ and $Z_{cs}(3985)$ states to pin down the $\tilde{g}_s^{cs}, \tilde{g}_a^{cs}, \tilde{g}_{sp}^{cs}$, and $\tilde{g}_{ap}^{cs}$. To determine the $\tilde{g}_s^c, \tilde{g}_a^c, \tilde{g}_{sp}^c$, and $\tilde{g}_{ap}^c$ in the Z_c sector, we need to select two observed Z_c states. Here, since the $Z_c(4020)$ is the HQS partner of the $Z_c(3900)$, if we use the experimental mass and width of $Z_c(3900)$ as inputs, then the resonance parameters of $Z_c(4020)$ can no longer be regarded as independent inputs.

Alternatively, we notice that the BELLE collaboration [4] reported a $Z_c(4050)$ state in the $\pi\chi_{c1}(1P)$ final states. Theoretically, this state has been discussed within the tetraquark [58–61], hadron-molecule [62–65], and triangle singularity [66] picture. For a more complete summary, see reviews [10,67]. The $Z_c(4050)$ is close to the $D^*\bar{D}^*$ threshold; due to the nonobservation of the $|DD^*, 1^{++}\rangle$ state, its HQS partner $|D^*D^*, 2^{++}\rangle$ should not exist either. Thus, we assume the $Z_c(4050)$ state is a resonance composed of the $D^*\bar{D}^*$ component with quantum number $J^{PC} = 0^{++}$. Then the selected observed Z_{cs} and Z_c states in sets 1 and 2 are

Set 1: $Z_{cs}(4000)|D\bar{D}_s^*;1^{+-}\rangle^{\sim}, \qquad Z_{cs}(3985)|D\bar{D}_s^*;1^{++}\rangle^{\sim},$

Set 2: $Z_c(3900)|D\bar{D}^*;1^{+-}\rangle, \qquad Z_c(4050)|D^*\bar{D}^*;0^{++}\rangle,$

respectively. The SU(3) breaking factor g_x is related to the effective potentials of the Z_c states and has not been determined yet, we fix the Λ at 1.0 GeV, then we run the g_x in a reasonable region; at the minimum χ^2, we obtain $g_x = 1.37$.

We present the Λ dependences of LECs extracted from the inputs of sets 1 and 2 in Fig. 2. As can be seen from Fig. 2, the LECs extracted from sets 1 and 2 have identical signs with comparable magnitudes. In the 0.8 GeV $\leq \Lambda \leq$ 1.4 GeV region, the parameters $\tilde{g}_s, \tilde{g}_a, \tilde{g}_{sp}$, and $\tilde{g}_{ap}$ have similar variation tendencies; this fact shows that the similarities of the LECs extracted from sets 1 and 2 have weak Λ dependences.

The results presented in Fig. 2 also show that the obtained $\tilde{g}_a$ and $\tilde{g}_{ap}$ in set 1 are different from that of set 2. Here, if we have appropriately handled the SU(3) breaking effect among the Z_c and Z_{cs} states, then the differences of the $\tilde{g}_a$ and $\tilde{g}_{ap}$ in sets 1 and 2 mainly depend on the inputs of the central values of the selected Z_c and Z_{cs} states. At present, we only use the central values of the experimental data to extract the LECs form sets 1 and 2, and it is difficult to include the experimental uncertainties of the masses and widths of the selected Z_{cs} and Z_c states into our analysis. The main reason is that if we include such uncertainties, the four LECs will also lie in the four solved
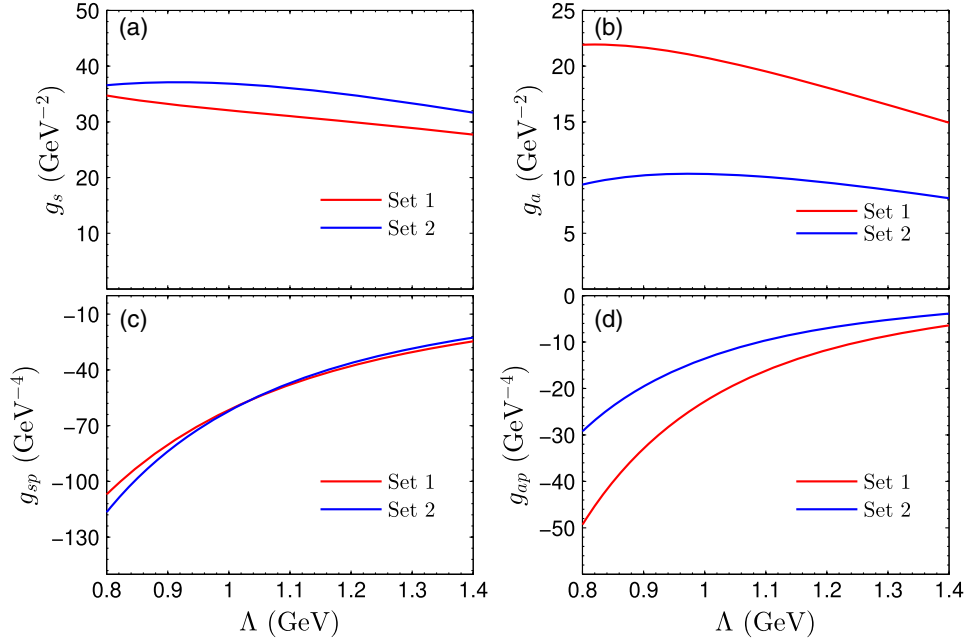
FIG. 2. The Λ dependences of the LECs (g_s, g_a, g_{sp}, g_{ap}) solved with the inputs from sets 1 and 2. The red lines and blue lines denote the LEC solved from sets 1 and 2, respectively.

regions, correspondingly. These solved regions may also extend in wide ranges, depending on the experimental uncertainties. Thus, comparing the four LEC wide ranges obtained from sets 1 and 2 cannot give a significant similarity hint between the Z_{cs} and Z_c states.

Instead, we perform a numerical experiment; i.e., we adjust one of the experimental inputs, then we check if the similarities of the LECs extracted from sets 1 and 2 can become better. We notice that the recent experiment from the BESIII collaboration reported the nonobservation of the $Z_{cs}(3985)$ in the $J/\Psi K$ final states [48]. Besides, they fitted a small excess of Z_{cs} over other components, the obtained mass and width are 4.044 ± 0.006 and 0.036 ± 0.016 GeV, respectively. The significance of this small excess is only 2.3σ. If such excess is related to a Z_{cs} state, it may correspond to the $Z_{cs}(4000)$ reported from the LHCb collaboration [6]. The resonance parameters of the $Z_{cs}(4000)$ from these two experiments are very different.

Here, we adopt the central value of the mass of $Z_{cs}(4000)$ from the LHCb, but treat the width of the $Z_{cs}(4000)$ as an adjustable parameter. We adjust the width of the $Z_{cs}(4000)$ and the SU(3) breaking factor g_x to find the minimum χ^2. We find that to obtain a minimum χ^2, the g_x is fixed at 1.27, and the width of the $Z_{cs}(4000)$ is adjusted to be 70 MeV. The results are presented in Fig. 3. As can be seen from Fig. 3, the LECs $\tilde{g}_s$, $\tilde{g}_a$, $\tilde{g}_{sp}$, and $\tilde{g}_{ap}$ extracted from the Z_c and Z_{cs} states [the width of the $Z_{cs}(4000)$ is fixed at 70 MeV] show very good consistencies in a relatively big Λ region. In this case, the resonance parameters of the observed Z_{cs} and Z_c states can be described simultaneously. In this framework, the

differences of the effective potentials of Z_{cs} and Z_c states can be described by only introducing an SU(3) breaking factor g_x. This result inspires us to believe that the constructed framework might be a promising solution for a unified description of the Z_{cs} and Z_c states.

IV. PREDICTIONS TO OTHER Z_{cs} AND Z_c STATES

In this section, we give our predictions for the rest of the Z_{cs} and Z_c states that are close to the thresholds of $D^{(*)}\bar{D}_s^{(*)}$ and $D^{(*)}\bar{D}^{(*)}$, respectively. We separately fit the LECs in the Z_{cs} and Z_c sectors with the inputs from sets 1 and 2 introduced in Sec. III C. Each set consists of four quantities, the masses and widths of the two Z_{cs} or Z_c states. Each mass or width includes three values, i.e., the experimental upper limit, central value, and lower limit. We consider different combinations of the three values of these four quantities to solve the corresponding LECs, and use the obtained LECs to calculate the lower and upper limits of the predicted Z_{cs} or Z_c state. The results are presented in Table IV.

In Table IV, we label the experimental inputs with superscript "a." As shown in Table IV, in the Z_c sector, except the input states in set 2, we only find a $Z_c(4020)$ state; this state shares identical effective potential with that of the $Z_c(3900)$ in the HQS limit, they have comparable $\delta_{M-M_{\mathrm{Tr}}}$ values and widths. As listed in Table I, the LHCb collaboration reported [7] a $Z_c(4100)$ in the $\eta_c\pi$ final states; the possible underlying structure of this state is still under debate [37,67–75]. The J^{PC} number of this state could be 0^{++}, if we consider the large uncertainties of the mass and
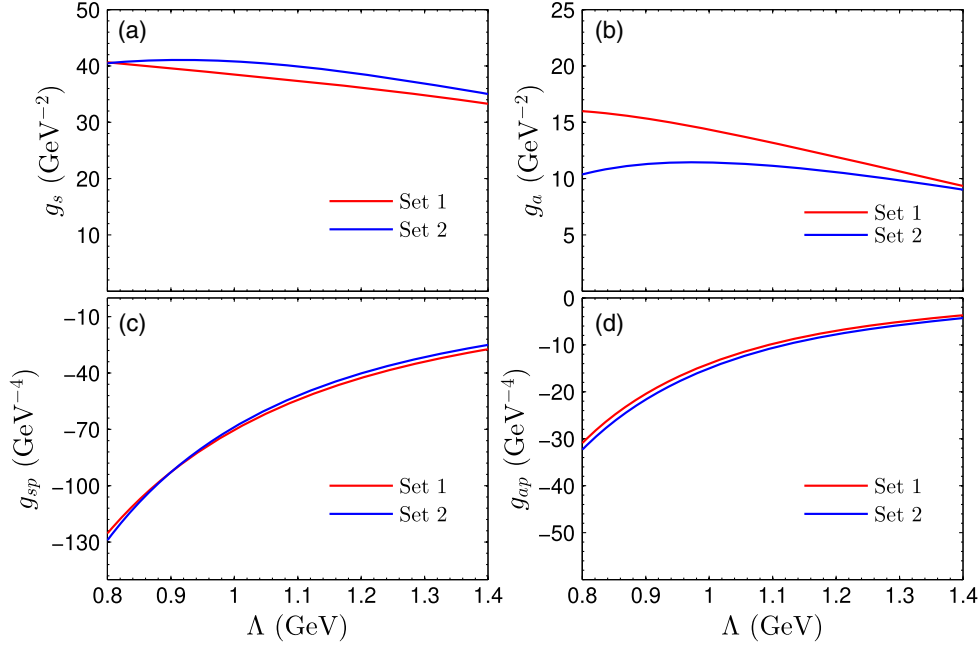
FIG. 3. The Λ dependences of the LECs (g_s, g_a, g_{sp}, g_{ap}) solved with the inputs from sets 1 and 2. Instead of using the experimental width, we fix the width of the $Z_{cs}(4000)$ at 70 MeV in set 1. The red lines and blue lines denote the LEC solved from sets 1 and 2, respectively.

width of $Z_c(4100)$, the $Z_c(4100)$ and $Z_c(4050)$ could be the same state. Besides, if we tentatively assign the $Z_c(4055)$ [9] and $Z_c(4020)$ as the same state, then our framework could give a unified description of the observed Z_c states (as listed in Table I) that are close to the $D^{(*)}\bar{D}^{(*)}$ thresholds.

As shown in Table IV, comparing to the Z_c sector, in the Z_{cs} sector, we obtain three extra Z_{cs} states, i.e., the $|D\bar{D}_s; 0^{+\widetilde{+}}\rangle$, $|D\bar{D}_s^*; 1^{+\widetilde{+}}\rangle$, and $|D^*\bar{D}_s^*; 2^{+\widetilde{+}}\rangle$ states. Because of the SU(3) breaking effect, these three states do not have their SU(3) flavor Z_c partners. We predict two $J^{PC} = 0^{+\widetilde{+}}$ Z_{cs} states that are composed of the $D\bar{D}_s$ and $D^*\bar{D}_s^*$ components; they are all broad with widths around 80 and 160 MeV, respectively. The $D\bar{D}_s$ and $\eta_c K$ are the possible decay channels for the $|D\bar{D}_s; 0^{+\widetilde{+}}\rangle$ state. Similarly,

the $D\bar{D}_s$, $D^*\bar{D}_s^*$, and $\eta_c K$ are the possible decay channels for the $|D^*\bar{D}_s^*; 0^{+\widetilde{+}}\rangle$ state. We notice that the LHCb collaboration has measured the $\eta_c K$ invariant spectrum in the $B^0 \to \eta_c K^+\pi^-$ process [7]. They found that without introducing some extra Z_{cs} resonance contributions, it is possible to describe the $m(\eta_c K)$ and $m(K\pi)$ distribution well with the $K\pi$ contributions alone. However, we notice that there exists a dip at about 4050 MeV in the $\eta_c K$ invariant spectrum [7]. The obtained results led us to conjecture if such a dip could relate to the splitting of the predicted two $0^{+\widetilde{+}}$ states. If these two states do exist, we also suggest to look for them in the invariant spectra of the $D\bar{D}_s$ and $D^*\bar{D}_s^*$ final states.

As shown in Table IV, the ($|D\bar{D}_s^*; 1^{+\widetilde{+}}\rangle$, $|\bar{D}^*\bar{D}_s^*; 2^{+\widetilde{+}}\rangle$) and ($|D\bar{D}_s^*; 1^{+\widetilde{-}}\rangle$, $|\bar{D}^*\bar{D}_s^*; 1^{+\widetilde{-}}\rangle$) are the two pairs of the

TABLE IV. Our predictions for the possible Z_c and Z_{cs} resonances. All the results are in units of MeV.

Threshold	State	Mass	Width	Threshold	State	Mass	Width
3734.4	$\|D\bar{D}; 0^{++}\rangle$	$\cdots$	$\cdots$	3835.6	$\|D\bar{D}_s; 0^{+\widetilde{+}}\rangle$	3879.7 ± 20.9	80.5 ± 19.0
3875.8	$\|D\bar{D}^*; 1^{++}\rangle$	$\cdots$	$\cdots$	3979.3	$\|D\bar{D}_s^*; 1^{+\widetilde{+}}\rangle$	[a]3985.2 ± 2.6	[a]$13.8^{+9.4}_{-7.2}$
3875.8	$\|D\bar{D}^*; 1^{+-}\rangle$	[a]3887.1 ± 2.6	[a]28.6 ± 2.6	3979.3	$\|D\bar{D}_s^*; 1^{+\widetilde{-}}\rangle$	[a]$4003.0^{+7.2}_{-15.2}$	[a]131.0 ± 30.0
4017.1	$\|D^*\bar{D}^*; 0^{++}\rangle$	[a]$4051.0^{+24.0}_{-43.0}$	[a]$82.0^{+52.0}_{-28.0}$	4120.7	$\|D^*\bar{D}_s^*; 0^{+\widetilde{+}}\rangle$	4134.1 ± 5.8	163.0 ± 25.0
4017.1	$\|D^*\bar{D}^*; 1^{+-}\rangle$	4022.2 ± 2.6	18.5 ± 3.2	4120.7	$\|D^*\bar{D}_s^*; 1^{+\widetilde{-}}\rangle$	4142.9 ± 7.0	125.4 ± 44.6
4017.1	$\|D^*\bar{D}^*; 2^{++}\rangle$	$\cdots$	$\cdots$	4120.7	$\|D^*\bar{D}_s^*; 2^{+\widetilde{+}}\rangle$	4121.8 ± 1.0	8.8 ± 4.2

[a]Denotes experimental inputs introduced in sets 1 and 2 for the Z_{cs} and Z_c states, respectively.

HQS partners. The states in each pair share comparable $\delta_{M-M_{\mathrm{Tr}}}$ values and widths. Among them, the predicted $|\bar{D}^*\bar{D}_s^*; 1^{+\widetilde{-}}\rangle$ may correspond to the $Z_{cs}(4220)$ if we consider the large experimental uncertainties of the $Z_{cs}(4220)$ from the LHCb collaboration [6]. Besides, the predicted $|\bar{D}^*\bar{D}_s^*; 2^{++}\rangle$ state may correspond to the $Z_{cs}(4123)$ state reported from the BESIII collaboration [8]. This state has already been discussed in various models [25,28,38,43,46,47,76–80]; nevertheless, this state still needs further confirmation due to its low significance. Thus, we also give a unified description of the observed Z_{cs} (as listed in Table I) states that are close to the $D^{(*)}\bar{D}_s^{(*)}$ thresholds. Further measurements of the Z_{cs} states will provide important inputs to our model, and will also provide important clues to test our theory.

V. SUMMARY

To summarize, in this work, we propose a possible framework to describe the observed Z_c and Z_{cs} states (listed in Table I) that are close to the $D^{(*)}\bar{D}^{(*)}$ and $D^{(*)}\bar{D}_s^{(*)}$ thresholds, respectively.

We construct the effective potentials of the Z_{cs} and Z_c states by analogy with the effective potentials of the LO and NLO $N\bar{N}$ interactions. In the SU(3) flavor limit, according to the expressions of the effective potentials of the $N\bar{N}$ interactions, we reduce the LECs describing the effective potentials of the Z_c and Z_{cs} states into four parameters, i.e., $\tilde{g}_s$, $\tilde{g}_a$, $\tilde{g}_{sp}$, and $\tilde{g}_{ap}$. In addition, to identify the differences between the Z_c and Z_{cs} states, we further introduce an SU(3) breaking factor g_x; this factor is expected to be greater than 1 if we consider the different masses of the exchanged light mesons with different isospins.

First, we determine the LECs $\tilde{g}_s$, $\tilde{g}_a$, $\tilde{g}_{sp}$, and $\tilde{g}_{ap}$ from the inputs of the experimental masses and widths of the $Z_{cs}(4000)$ and $Z_{cs}(3985)$ states. They are assumed to be the $J^{P\tilde{C}} = 1^{+\widetilde{-}}$ and 1^{++} states, respectively. Then we directly adopt the obtained four LECs to calculate the $J^{PC} = 1^{+-}$ and 1^{++} states that are composed of the $D^{(*)}\bar{D}^*$. We run the undetermined parameter g_x in the effective potentials of the Z_c states and show that a considerable SU(3) breaking effect will lead the absences of the $|D\bar{D}^*; 1^{++}\rangle$ and $|D^*\bar{D}^*; 2^{++}\rangle$ states; these two states should be the SU(3) partners of the $Z_{cs}(3985)$ and $Z_{cs}(4123)$ [the $Z_{cs}(4123)$ still need further confirmation], respectively.

Besides, we also show that the SU(3) breaking effect will also reduce the width of the $|D\bar{D}^*; 1^{+-}\rangle$ state. This can qualitatively explain the large width difference between the $Z_c(3900)$ and $Z_{cs}(4000)$.

Then we compare the similarities between the Z_{cs} and Z_c states in another scheme. We determine the LECs from the inputs of the observed Z_{cs} (set 1) and Z_c (set 2) states separately. Then we compare the similarities of the LECs extracted from these two sets. In this scheme, we fix the SU(3) breaking factor by finding the minimum χ^2 at $\Lambda = 1.0$ GeV. We show that the LECs obtained from sets 1 and 2 are very close to each other, and this similarity has weak Λ dependence. In particular, if we adjust the width of the mass of the $Z_{cs}(4000)$ to be 70 MeV, then the LECs extracted from sets 1 and 2 are almost the same, and have very weak Λ dependences. This result led us to believe that this framework might be a promising solution for a unified description of the Z_c and Z_{cs} states. Thus, further measurements on the resonance parameters of the observed Z_c and Z_{cs} states will provide important guidance to our calculation.

We also check the other possible resonances in the Z_{cs} and Z_c sectors. Comparing to the calculated Z_c sector, the results in the Z_{cs} sector may exist three extra Z_{cs} states, i.e., the $|D\bar{D}_s; 0^{++}\rangle$, $|D\bar{D}_s^*; 1^{++}\rangle$, and $|D^*\bar{D}_s^*; 2^{++}\rangle$ states. The emergence of these three states is the consequence of the SU(3) breaking effect. Besides, we suggest to look for the $|D\bar{D}_s; 0^{++}\rangle$ state in the $D\bar{D}_s$ and $\eta_c K$ final states, and look for the $|D^*\bar{D}_s^*; 0^{++}\rangle$ state in the $D\bar{D}_s$, $D^*\bar{D}_s^*$, and $\eta_c K$ final states. With some reasonable assumptions, we place all the observed Z_{cs} and Z_c states into our framework. We hope that further explorations and measurements on these discussed Z_{cs} and Z_c states in the future can test our theory.

[1] R. L. Workman *et al.* (Particle Data Group), Prog. Theor. Exp. Phys. **2022,** 083C01 (2022).

[2] M. Ablikim *et al.* (BESIII Collaboration), Phys. Rev. Lett. **126,** 102001 (2021).

[3] M. Ablikim *et al.* (BESIII Collaboration), Phys. Rev. Lett. **129,** 112003 (2022).

[4] R. Mizuk *et al.* (Belle Collaboration), Phys. Rev. D **78,** 072004 (2008).

[5] R. Aaij *et al.* (LHCb Collaboration), Phys. Rev. Lett. **131,** 131901 (2023).

[6] R. Aaij *et al.* (LHCb Collaboration), Phys. Rev. Lett. **127,** 082001 (2021).

[7] R. Aaij *et al.* (LHCb Collaboration), Eur. Phys. J. C **78,** 1019 (2018).

[8] M. Ablikim *et al.* (BESIII Collaboration), Chin. Phys. C **47,** 033001 (2023).

[9] X. L. Wang *et al.* (Belle Collaboration), Phys. Rev. D **91,** 112007 (2015).

[10] H. X. Chen, W. Chen, X. Liu, and S. L. Zhu, Phys. Rep. **639,** 1 (2016).

[11] R. F. Lebed, R. E. Mitchell, and E. S. Swanson, Prog. Part. Nucl. Phys. **93,** 143 (2017).

[12] A. Esposito, A. Pilloni, and A. D. Polosa, Phys. Rep. **668,** 1 (2017).

[13] A. Hosaka, T. Iijima, K. Miyabayashi, Y. Sakai, and S. Yasui, Prog. Theor. Exp. Phys. **2016,** 062C01 (2016).

[14] F. K. Guo, C. Hanhart, U. G. Meißner, Q. Wang, Q. Zhao, and B. S. Zou, Rev. Mod. Phys. **90,** 015004 (2018); **94,** 029901(E) (2022).

[15] A. Ali, J. S. Lange, and S. Stone, Prog. Part. Nucl. Phys. **97,** 123 (2017).

[16] Y. R. Liu, H. X. Chen, W. Chen, X. Liu, and S. L. Zhu, Prog. Part. Nucl. Phys. **107,** 237 (2019).

[17] N. Brambilla, S. Eidelman, C. Hanhart, A. Nefediev, C. P. Shen, C. E. Thomas, A. Vairo, and C. Z. Yuan, Phys. Rep. **873,** 1 (2020).

[18] W. Lucha, D. Melikhov, and H. Sazdjian, Prog. Part. Nucl. Phys. **120,** 103867 (2021).

[19] S. Chen, Y. Li, W. Qian, Z. Shen, Y. Xie, Z. Yang, L. Zhang, and Y. Zhang, Front. Phys. **18,** 44601 (2023).

[20] H. X. Chen, W. Chen, X. Liu, Y. R. Liu, and S. L. Zhu, Rep. Prog. Phys. **86,** 026201 (2023).

[21] L. Meng, B. Wang, G. J. Wang, and S. L. Zhu, Phys. Rep. **1019,** 1 (2023).

[22] M. Ablikim *et al.* (BESIII Collaboration), Phys. Rev. Lett. **119,** 072001 (2017).

[23] A. Bondar, in *9th International Workshop on Charm Physics* (Novosibirsk, Russia, 2018), https://indico.inp.nsk.su/event/10/contributions/292/attachments/199/231/A.Bondar-Charm18.pdf.

[24] R. Chen and Q. Huang, Phys. Rev. D **103,** 034008 (2021).

[25] M. J. Yan, F. Z. Peng, M. Sánchez Sánchez, and M. Pavon Valderrama, Phys. Rev. D **104,** 114025 (2021).

[26] H. X. Chen, Phys. Rev. D **105,** 094003 (2022).

[27] Q. Wu, D. Y. Chen, W. H. Qin, and G. Li, Eur. Phys. J. C **82,** 520 (2022).

[28] M. L. Du, M. Albaladejo, F. K. Guo, and J. Nieves, Phys. Rev. D **105,** 074018 (2022).

[29] L. Meng, B. Wang, G. J. Wang, and S. L. Zhu, Sci. Bull. **66,** 2065 (2021).

[30] Q. Y. Zhai, M. Z. Liu, J. X. Lu, and L. S. Geng, Phys. Rev. D **106,** 034026 (2022).

[31] J. B. Cheng, B. L. Huang, Z. Y. Lin, and S. L. Zhu, Eur. Phys. J. C **83,** 1071 (2023).

[32] U. Özdem and A. K. Yıldırım, Phys. Rev. D **104,** 054017 (2021).

[33] U. Özdem and K. Azizi, Eur. Phys. J. Plus **136,** 968 (2021).

[34] Z. G. Wang, Int. J. Mod. Phys. A **36,** 2150107 (2021).

[35] Z. G. Wang, Chin. Phys. C **45,** 073107 (2021).

[36] Z. G. Wang, Chin. Phys. C **46,** 123106 (2022).

[37] G. Yang, J. Ping, and J. Segovia, Phys. Rev. D **104,** 094035 (2021).

[38] X. Jin, Y. Wu, X. Liu, H. Huang, J. Ping, and B. Zhong, Eur. Phys. J. C **81,** 1108 (2021).

[39] L. Maiani, A. D. Polosa, and V. Riquer, Sci. Bull. **66,** 1616 (2021).

[40] Y. H. Wang, J. Wei, C. S. An, and C. R. Deng, Chin. Phys. Lett. **40,** 021201 (2023).

[41] P. P. Shi, F. Huang, and W. L. Wang, Phys. Rev. D **103,** 094038 (2021).

[42] M. Karliner and J. L. Rosner, Phys. Rev. D **104,** 034033 (2021).

[43] S. Han and L. Y. Xiao, Phys. Rev. D **105,** 054008 (2022).

[44] Z. H. Cao, W. He, and Z. F. Sun, Phys. Rev. D **107,** 014017 (2023).

[45] X. Luo and S. X. Nakamura, Phys. Rev. D **107,** L011504 (2023).

[46] P. G. Ortega, D. R. Entem, and F. Fernandez, Phys. Lett. B **818,** 136382 (2021).

[47] J. F. Giron, R. F. Lebed, and S. R. Martinez, Phys. Rev. D **104,** 054001 (2021).

[48] M. Ablikim *et al.* (BESIII Collaboration), Phys. Rev. Lett. **131,** 211902 (2023).

[49] X. W. Kang, J. Haidenbauer, and U. G. Meißner, J. High Energy Phys. 02 (2014) 113.

[50] K. Chen, Z. Y. Lin, and S. L. Zhu, Phys. Rev. D **106,** 116017 (2022).

[51] J. Haidenbauer, X. W. Kang, and U. G. Meißner, Nucl. Phys. **A929,** 102 (2014).

[52] X. W. Kang, J. Haidenbauer, and U. G. Meißner, Phys. Rev. D **91,** 074003 (2015).

[53] J. Haidenbauer, C. Hanhart, X. W. Kang, and U. G. Meißner, Phys. Rev. D **92,** 054032 (2015).

[54] D. B. Leinweber, A. W. Thomas, and R. D. Young, Phys. Rev. Lett. **92,** 242002 (2004).

[55] P. Wang, D. B. Leinweber, A. W. Thomas, and R. D. Young, Phys. Rev. D **75,** 073012 (2007).

[56] S. X. Nakamura and J. J. Wu, Phys. Rev. D **108,** L011501 (2023).

[57] E. Epelbaum, J. Gegelia, and U. G. Meißner, Nucl. Phys. **B925,** 161 (2017).

[58] D. Ebert, R. N. Faustov, and V. O. Galkin, Eur. Phys. J. C **58,** 399 (2008).

[59] S. Patel, M. Shah, and P. C. Vinodkumar, Eur. Phys. J. A **50,** 131 (2014).

[60] C. Deng, J. Ping, H. Huang, and F. Wang, Phys. Rev. D **92,** 034027 (2015).

[61] Z. G. Wang, Commun. Theor. Phys. **63,** 466 (2015).

[62] X. Liu, Z. G. Luo, Y. R. Liu, and S. L. Zhu, Eur. Phys. J. C **61,** 411 (2009).

[63] Y. R. Liu and Z. Y. Zhang, Phys. Rev. C **80,** 015208 (2009).
[64] G. J. Ding, Phys. Rev. D **79,** 014001 (2009).
[65] S. H. Lee, K. Morita, and M. Nielsen, Phys. Rev. D **78,** 076001 (2008).
[66] S. X. Nakamura, Phys. Rev. D **100,** 011504 (2019).
[67] R. M. Albuquerque, J. M. Dias, K. P. Khemchandani, A. Martínez Torres, F. S. Navarra, M. Nielsen, and C. M. Zanetti, J. Phys. G **46,** 093002 (2019).
[68] Z. G. Wang, Eur. Phys. J. C **78,** 933 (2018).
[69] M. B. Voloshin, Phys. Rev. D **98,** 094028 (2018).
[70] Q. Zhao, arXiv:1811.05357.
[71] J. Wu, X. Liu, Y. R. Liu, and S. L. Zhu, Phys. Rev. D **99,** 014037 (2019).
[72] X. Cao and J. P. Dai, Phys. Rev. D **100,** 054004 (2019).

[73] H. Sundu, S. S. Agaev, and K. Azizi, Eur. Phys. J. C **79,** 215 (2019).
[74] X. Cao and Z. Yang, Eur. Phys. J. C **82,** 161 (2022).
[75] V. Baru, E. Epelbaum, A. A. Filin, C. Hanhart, and A. V. Nefediev, Phys. Rev. D **105,** 034014 (2022).
[76] Q. N. Wang, W. Chen, and H. X. Chen, Chin. Phys. C **45,** 093102 (2021).
[77] N. Ikeno, R. Molina, and E. Oset, Phys. Rev. D **105,** 014012 (2022); **106,** 099905(E) (2022).
[78] L. Meng, B. Wang, and S. L. Zhu, Phys. Rev. D **102,** 111502 (2020).
[79] Z. Yang, X. Cao, F. K. Guo, J. Nieves, and M. P. Valderrama, Phys. Rev. D **103,** 074029 (2021).
[80] Z. M. Ding, H. Y. Jiang, D. Song, and J. He, Eur. Phys. J. C **81,** 732 (2021).